

## A Quasar Pair Catalog Compiled from DESI DR1

LIANG JING <sup>1,2</sup> QIHANG CHEN<sup>†</sup> <sup>1,2</sup> ZHUOJUN DENG <sup>1,2</sup> XINGYU ZHU <sup>1,2</sup> HU ZOU <sup>3</sup> AND JIANGHUA WU<sup>†</sup> <sup>1,2</sup>

<sup>1</sup>*School of Physics and Astronomy, Beijing Normal University, Beijing, 100875, China*

<sup>2</sup>*Institute for Frontier in Astronomy and Astrophysics, Beijing Normal University, Beijing, 102206, China*

<sup>3</sup>*Key Laboratory of Optical Astronomy, National Astronomical Observatories, Chinese Academy of Sciences, Beijing 100012, China*

### ABSTRACT

We present a catalog of quasar pairs (QPs) constructed from the DESI DR1 quasar sample, comprising 1.6 million spectroscopically confirmed quasars. By performing a redshift-dependent self-matching process and applying physical constraints on projected separation ( $\lesssim 110$  kpc) and line-of-sight velocity difference ( $\lesssim 2000$  km/s), we identified 1,842 candidate quasar pairs. Each pair is spectroscopically confirmed, enabling reliable redshift and velocity measurements. We visually classified these systems using DESI Legacy Imaging and SPARCL spectral data into four categories: QP (projected quasar pairs), QPC (quasar pair candidates), LQC (lensed quasar candidates), and Uncertain. We find that the redshift distribution peaks at  $z \sim 1\text{--}2.5$  and that 64.3% of QPs have  $|\Delta v| < 600$  km/s, indicating that many systems may be physically bound. The catalog offers a statistically meaningful sample for future studies of dual AGNs, lensing events, and quasar clustering.

*Keywords:* Quasar Pair (18)— Lensed Quasar (4) — DESI (26)

### 1. INTRODUCTION

Supermassive black holes (SMBHs) are recognized as fundamental components of massive galaxies, with their growth closely intertwined with the evolution of their host systems. Accretion onto SMBHs, manifested as active galactic nuclei (AGNs), serves as a key tracer of black hole growth and galaxy assembly (P. F. Hopkins et al. 2005; P. R. Capelo et al. 2017; L. Blecha et al. 2018). Understanding when and how AGN activity is triggered, and how it evolves across different stages of galaxy evolution, is essential for constructing a comprehensive picture of cosmic structure formation (T. M. Heckman & P. N. Best 2014).

Galaxy mergers are transformative events that fundamentally reshape the structure, gas distribution, star formation, and overall evolutionary trajectories of galaxies (J. E. Barnes & L. E. Hernquist 1991; J. E. Barnes & L. Hernquist 1996; J. C. Mihos & L. Hernquist 1994, 1996; P. F. Hopkins et al. 2005; T. J. Cox et al. 2008; P. R. Capelo et al. 2015; L. Blecha et al. 2018). They are widely believed to play a pivotal role in triggering AGN activity. As these colossal systems interact, gravitational forces instigate intense bursts of star formation and drive gas and dust toward their central regions,

thereby fueling the activity of supermassive black holes (J. E. Barnes & L. E. Hernquist 1991; J. C. Mihos & L. Hernquist 1994, 1996; T. J. Cox et al. 2008; P. R. Capelo et al. 2017; L. Blecha et al. 2018). This process leads to the emergence of dual quasar systems, where two active nuclei are ignited within a single merging galaxy, with their eventual coalescence anticipated to generate detectable gravitational waves (L. Z. Kelley et al. 2017; G. Agazie et al. 2023). Simulations further predict that during specific merger stages, dual or multiple AGN systems—where two or more SMBHs are simultaneously accreting—can emerge and remain active over timescales of tens to hundreds of millions of years (S. Van Wassenhove et al. 2012; N. Chen et al. 2023; R. W. Pfeifle et al. 2024).

In recent years, numerous efforts have been devoted to identifying and characterizing dual AGN systems (X. Liu et al. 2010, 2011; Y. Shen et al. 2011; M. Koss et al. 2012; X. Liu et al. 2013; J. M. Comerford et al. 2015; S. Satyapal et al. 2017; A. De Rosa et al. 2018; R. W. Pfeifle et al. 2019; M. Hou et al. 2019, 2020; A. De Rosa et al. 2023; R. S. Barrows et al. 2023). In parallel, a series of systematic, catalog-based studies have advanced the search for dual quasar systems (H.-C. Hwang et al. 2020; V. V. Makarov & N. J. Secrest 2023; C. Dawes et al. 2023; Q. Wu et al. 2024; Q. Chen et al. 2025). Multi-wavelength observations of these systems have revealed

complex interactions between merging galaxies and their central SMBHs, offering insights into both small-scale AGN triggering mechanisms and the broader context of large-scale structure formation (F. Müller-Sánchez et al. 2015; A. De Rosa et al. 2023). Despite their importance, the systematic identification of dual and multiple AGN systems remains observationally challenging. The total number of confirmed dual AGNs and dual quasars is still relatively small, only  $\sim 160$  quasar pairs with a transverse distance of less than 100 kpc are publicly confirmed to date (R. W. Pfeifle et al. 2024). Existing samples are often heterogeneous, being constructed from serendipitous discoveries, high-resolution imaging, or spatially resolved spectroscopy, and are typically biased toward specific merger stages or AGN luminosity regimes (R. W. Pfeifle et al. 2024). These constraints hinder robust statistical analyses and obscure the full diversity of dual AGN systems. To overcome these obstacles, it is imperative to pursue deeper, more homogeneous surveys and refine detection techniques, which will ultimately improve models of galaxy evolution and black hole growth.

Recently, the Dark Energy Spectroscopic Instrument (DESI) released its first data release (DR1), containing 1.6 million spectroscopically confirmed quasars (202 2025). With its large sky coverage, high spectral quality, and systematic target selection, DR1 offers a deep and statistically uniform quasar sample well suited for population studies. In this work, we perform a self-matching analysis of the DR1 quasar catalog to systematically search for projected quasar pairs and lensed quasars.

The paper is organized as follows. The spectroscopically confirmed quasar catalog exploited in this work and the method details are introduced in Sec.2. The derived quasar pairs and their classifications, as well as their basic statistical properties of, are described in Sec.3. Sec.4 discusses several remarkable and confusing quasar pairs. We summarize this work in Sec.5. A flat  $\Lambda$ CDM cosmology with  $\Omega_\Lambda = 0.7$ ,  $\Omega_M = 0.3$ , and  $H_0 = 70 \text{ km} \cdot \text{s}^{-1} \cdot \text{Mpc}^{-1}$  is adopted throughout this paper.

## 2. DATA AND METHOD

### 2.1. Data

The Dark Energy Spectroscopic Instrument (DESI) is a state-of-the-art multi-object spectrograph mounted on the Mayall 4-meter telescope at Kitt Peak National Observatory (KPNO) (M. Levi et al. 2013; DESI Collaboration et al. 2016; A. Dey et al. 2019; DESI Collaboration et al. 2022). Its first major data release, DESI-DR1, marks a significant milestone in spectroscopic surveys by providing high-quality spectra for millions of celestial objects, including 13.1M galaxies, 4M stars,

and 1.6M quasars (202 2025). In this work, we utilize the high-quality quasar spectroscopy provided in this release, which comprises quasars out to  $z \approx 4$  for 1,650,736 sources and 2,182,309 spectra<sup>4</sup>, offering an unparalleled resource for astrophysical research.

### 2.2. Method Details

In this study, we build upon the selection methods outlined in Q. Chen et al. (2025) to identify dual quasar candidates from the DESI-DR1 quasar catalog, which contains 1,650,736 sources and 2,182,309 spectra. Our approach begins by determining the angular separation corresponding to a physical scale of 110 kpc for each quasar, based on its redshift. This yields a redshift-dependent search radius that ensures the physical relevance of our candidate selection.

To define the projected separation constraint, we adopt the following criterion:

$$r_p \lesssim 110 \text{ kpc} \quad (1)$$

where  $r_p$  is the projected separation between two quasars. Using this dynamically scaled angular radius, we perform a self-matching procedure on the catalog, identifying all quasar pairs whose projected separations satisfy Equation 2.2. Following the self-cross matching, a deduplication process is applied to eliminate redundant pairings by retaining only one instance of each quasar pair (i.e., keeping either A–B or B–A), thereby refining our candidate list.

Next, we impose a radial velocity difference threshold to distinguish physically associated quasars from projected pairs (J. F. Hennawi et al. 2006, 2010). Specifically, we require:

$$|\Delta V_r| \lesssim 2000 \text{ km s}^{-1} \quad (2)$$

It accounts for peculiar velocities in dense environments, which can be as high as approximately  $\sim 500 \text{ km s}^{-1}$ , and for broad-line region redshift uncertainties of up to  $\sim 1500 \text{ km s}^{-1}$  due to blueshifted emission lines (G. T. Richards et al. 2002) This criterion is critical for distinguishing pairs that are likely at the same redshift—and therefore physically associated—from those that are merely chance alignments along the line of sight.

### 2.3. Target Classification

For the subset of quasar pairs that satisfy the same-redshift criterion, we perform a detailed visual inspection using imaging data from the ninth public data re-

<sup>4</sup> <https://data.desi.lbl.gov/public/dr1/survey/catalogs/dr1/QSO/iron/>

lease of the DESI Legacy Imaging Surveys (DESILS-DR9; H. Zou et al. 2017; A. Dey et al. 2019). The SPARCL tool<sup>5</sup> contains spectral data from SDSS-DR16, SDSS-DR17, BOSS-DR16 ( Abdurro'uf et al. 2022), and DESI-EDR ( DESI Collaboration et al. 2023). After matching with SPARCL using the x-match function in DataLab<sup>6</sup>, we can obtain a sparclid, which can then be used in SPARCL programs to retrieve various selectable information about the target object, such as redshift, data records, wavelength, flux, and much more. These spectral data enable the creation of detailed spectral plots for quasars, providing critical insights into their properties and behaviors.

This manual verification step is essential to assess the quality of the candidates. Pairs exhibiting clear and distinct nuclei in imaging data, along with significant differences in their spectral features, such as distinct emission or absorption line profiles, are flagged as potential dual quasar systems. In contrast, pairs showing lensing-like morphological features (e.g., arcs, symmetry, or alignment) and highly similar spectra are classified separately as lensed systems, as the spectral similarity is indicative of a single background quasar being gravitationally lensed. The entire workflow—from the initial angular separation calculation to the final visual verification—is summarized in the accompanying flowchart (see Figure 1). This comprehensive approach enhances the reliability of our candidate sample and lays the groundwork for future analyses of quasar pair populations and their physical properties.

Specifically, we divide the visually confirmed quasar pairs into four subcategories based on their morphological and spectroscopic characteristics:

- **QP (Quasar Pair):** Systems with angular separations  $\geq 2''$ , where neither a prominent lensing galaxy is visible between or near the components, and the two quasars exhibit noticeably different spectral features.
- **QPC (Quasar Pair Candidate):** Systems with angular separations  $< 2''$ , where the imaging clearly reveals two components without any apparent foreground lensing structure. Additionally, the flux ratio between the two spectra varies significantly with wavelength (visually inspected), suggesting the presence of two distinct sources.
- **LQC (Lensed Quasar Candidate):** Systems with either (1) angular separations  $\geq 2''$  and a

potential lensing galaxy present between the two components, combined with nearly constant flux ratios between the spectra; or (2) angular separations  $< 2''$  but exhibiting morphological or spectroscopic features indicative of gravitational lensing.

- **Uncertain:** Systems with poor image quality or ambiguous structure, where the components appear blended or possibly a single object.

### 3. QUASAR PAIR CATALOG

The final quasar pair catalog comprises 1,842 systems that satisfy both the projected separation and line-of-sight velocity criteria. Each pair consists of two quasars with spectroscopic confirmation, ensuring reliable redshift measurements for all sources. To identify previously studied sources within our sample, we cross-matched our catalog with the excellent work of the Big Multi-AGN Catalog (Big MAC; R. W. Pfeifle et al. 2024). By requiring both components (A and B) of each system to have positional matches within 1 arcsecond, we identified 23 overlapping systems. For reference, these matches are flagged in our final catalog table. The column descriptions of the catalog are summarized in Table 3, and the full catalog can be accessed at [https://github.com/astroliang/DESI\\_DR1\\_QP](https://github.com/astroliang/DESI_DR1_QP).

Here, we present one example for each classification.

#### 3.1. Quasar Pair

As shown in Figure 2, in system J0145+0024, the two quasars exhibit a relatively large angular separation, with no obvious intervening lensing structure between them, and their spectral features are clearly distinct.

#### 3.2. Quasar Pair Candidate

As shown in Figure 3, system J0118–0104 shows two quasars with a small angular separation, close to the DESI fiber diameter ( $1.5''$ ), which poses observational challenges. However, it is still a strong candidate for a quasar pair.

#### 3.3. Lensed quasar candidates

As shown in Figure 4, system J0941+0518 appears to have a massive, bright red galaxy situated between the two quasars, and the spectral features of the quasars are remarkably similar. These characteristics suggest a gravitational lensing configuration, and we therefore classify it as a lensed quasar candidate.

#### 3.4. Uncertain

As shown in Figure 5, system J0032+3021 shows two nearly identical quasar spectra at the same redshift, with

<sup>5</sup> <https://astroparcl.datalab.noirlab.edu/>

<sup>6</sup> <https://datalab.noirlab.edu/>

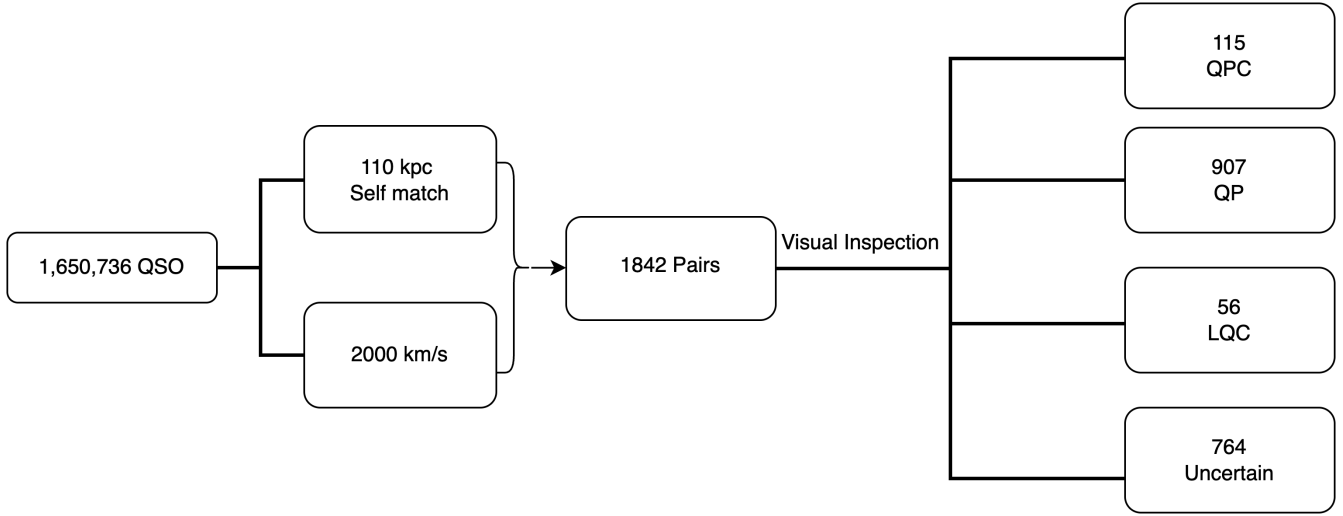


**Figure 1.** Flowchart of the quasar pair catalog selection process.

**Table 1.** Column descriptions of the quasar pair catalog.

Column	Description	Column	Description
System	System coordinate name	DEC_B	Declination of QSO B (deg)
SysCenterName	Complete system coordinate name	RA_B_sixa	Right Ascension of QSO B (sexagesimal)
TARGETID_A	DESI target ID of QSO A	DEC_B_sixa	Declination of QSO B (sexagesimal)
CoordUqName_A	Coordinate name of QSO A	Z_B	Redshift of QSO B
RA_A	Right Ascension of QSO A (deg)	ZERR_B	Redshift uncertainty of QSO B
DEC_A	Declination of QSO A (deg)	ZWARN_B	Redshift warning flag for QSO B
RA_A_sixa	Right Ascension of QSO A (sexagesimal)	FLUX_G_B	G-band flux of QSO B
DEC_A_sixa	Declination of QSO A (sexagesimal)	FLUX_R_B	R-band flux of QSO B
Z_A	Redshift of QSO A	FLUX_Z_B	Z-band flux of QSO B
ZERR_A	Redshift uncertainty of QSO A	FLUX_W1_B	WISE W1-band flux of QSO B
ZWARN_A	Redshift warning flag for QSO A	FLUX_W2_B	WISE W2-band flux of QSO B
FLUX_G_A	G-band flux of QSO A	FLUX_IVAR_G_B	Inverse variance of G-band flux (B)
FLUX_R_A	R-band flux of QSO A	FLUX_IVAR_R_B	Inverse variance of R-band flux (B)
FLUX_Z_A	Z-band flux of QSO A	FLUX_IVAR_Z_B	Inverse variance of Z-band flux (B)
FLUX_W1_A	WISE W1-band flux of QSO A	FLUX_IVAR_W1_B	Inverse variance of W1 flux (B)
FLUX_W2_A	WISE W2-band flux of QSO A	FLUX_IVAR_W2_B	Inverse variance of W2 flux (B)
FLUX_IVAR_G_A	Inverse variance of G-band flux (A)	MORPHTYPE_B	Morphological type of QSO B
FLUX_IVAR_R_A	Inverse variance of R-band flux (A)	SPECTYPE_B	Spectral classification of QSO B
FLUX_IVAR_Z_A	Inverse variance of Z-band flux (A)	LASTNIGHT_B	Observation date of QSO B
FLUX_IVAR_W1_A	Inverse variance of W1-band flux (A)	Sep_AB	Angular separation between QSO A and B
FLUX_IVAR_W2_A	Inverse variance of W2-band flux (A)	110kpc_seplim_zA	Angular scale of 110 kpc at z_A
MORPHTYPE_A	Morphological type of QSO A	110kpc_seplim_zB	Angular scale of 110 kpc at z_B
SPECTYPE_A	Spectral classification of QSO A	delta_vr	Velocity difference along the line of sight (km/s)
LASTNIGHT_A	Observation date of QSO A	rp_zA	Projected distance (A–B) calculated from z_A
TARGETID_B	DESI target ID of QSO B	rp_zB	Projected distance (A–B) calculated from z_B
CoordUqName_B	Coordinate name of QSO B	match_type	Result after with the Big MAC
RA_B	Right Ascension of QSO B (deg)	Classify	Classification after visual inspection

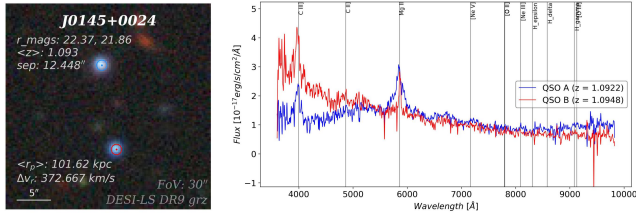


**Figure 2.** The two quasars exhibit a relatively large angular separation, with no obvious massive object between them to serve as a gravitational lens, making this system a likely QP. Their spectra are clearly distinct: quasar B shows prominent narrow emission lines, and the overall spectral slopes of the two sources differ, further supporting their independent nature.

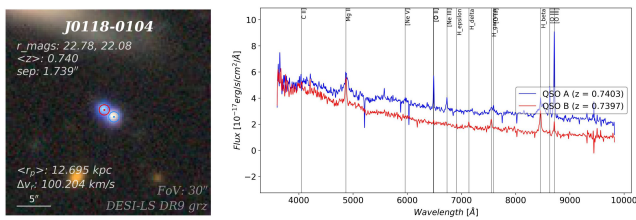


**Figure 3.** The two quasars exhibit a relatively small angular separation, with no obvious intervening lensing structure between them. Their angular separation is close to the DESI fiber diameter ( $1.5''$ ), which poses observational challenges, yet the lack of lensing features and their distinct spectral signatures suggest that this system is still a strong candidate for a projected quasar pair.

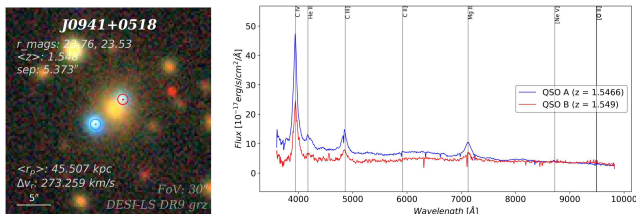


**Figure 4.** The two quasars have nearly identical spectral features, suggesting they may be multiple images of the same background source. A bright, red galaxy is clearly visible between them, likely serving as the lensing object. Although quasar B shows some absorption line features, this may be due to its alignment with the foreground galaxy, such that the line of sight passes through a relatively diffuse or unobscured region of the lens. Taken together, the morphological alignment and spectral similarity strongly support the classification of this system as a lensed quasar candidate.

an angular separation ( $1.11''$ ) smaller than the DESI fiber diameter. The imaging does not clearly resolve two distinct sources, suggesting this may be a duplicate observation rather than a true quasar pair. We therefore classify it as Uncertain.

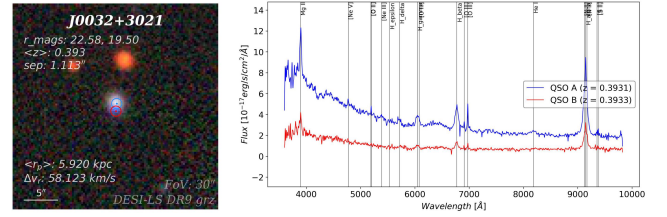


**Figure 5.** The two quasars have spectra with nearly identical redshifts and spectral features. The angular separation between the two components is only  $1.11''$ , which is smaller than the DESI fiber diameter ( $1.5''$ ). Given this small separation and the high degree of spectral similarity, it is plausible that the system represents a duplicate observation of the same source rather than a true quasar pair. The imaging also does not show two clearly resolved nuclei. Therefore, we classify this system as Uncertain, pending higher-resolution imaging or spectroscopic confirmation.

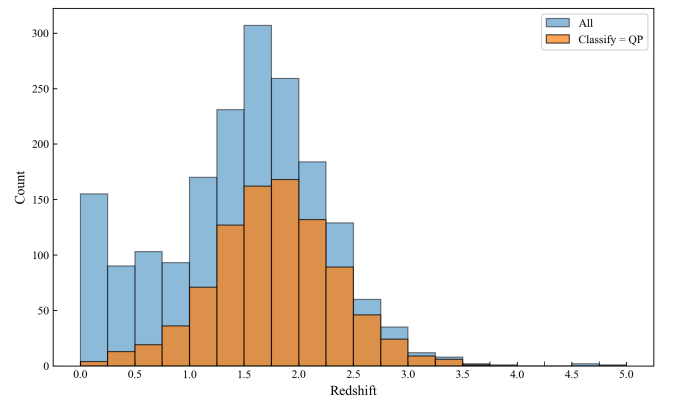


**Figure 6.** Redshift distribution of all quasar pair candidates (blue) and those classified as projected quasar pairs (QP; orange). The horizontal axis represents redshift, and the vertical axis shows the number of systems in each bin. The QP sample is primarily concentrated in the redshift range  $z \sim 1-2.5$ .

#### 4. DISCUSSIONS AND PROSPECTS

We analyzed the redshift and projected separation distributions of our quasar pair sample, as shown in Figure 6 and 7. The redshift distribution reveals that the majority of pairs are concentrated in the range  $z \sim 1-2.5$ , regardless of whether we include the full sample or restrict the analysis to the cleaner subset of QP. This suggests that quasars in this redshift range may be more likely to reside in the early, pre-merger stages of galaxy interaction.

In terms of projected separation, the number of quasar pairs remains relatively constant beyond  $\sim 20$  kpc, with no clear dependence on distance. This flat distribution may indicate a relatively long-lived or stable pre-merger phase during which the quasars remain physically as-

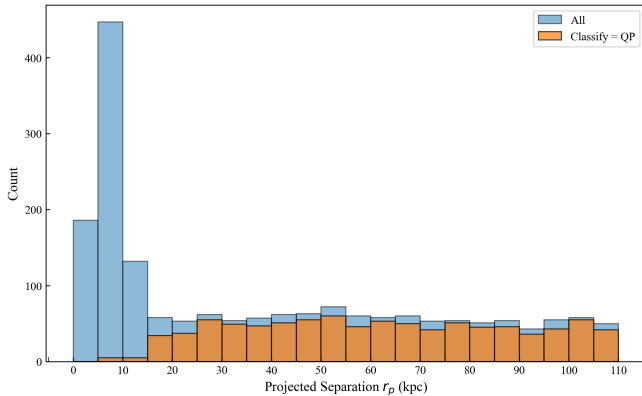


**Figure 7.** Distribution of projected separations  $r_p$  (in kpc) for the same two samples. A significant excess of systems with  $r_p < 10$  kpc is observed in the full sample, likely due to duplicate observations or unresolved sources, which are minimized in the QP subset.

sociated but not yet dynamically coalescing. However, given that the full sample includes systems classified as Uncertain, which may be contaminated by repeated observations of single sources, we focus our analysis on the cleaner subset of QPs to minimize such effects. A more detailed analysis—possibly incorporating merger time scales and selection effects—is needed to draw robust conclusions.

In addition, previous studies have suggested that the commonly adopted threshold of 2000 km/s for line-of-sight velocity differences may be too generous for identifying physically associated systems (X. Ji et al. 2024). To address this, we also calculated the fraction of QP systems with  $|\Delta v| < 600$  km/s. As shown in Figure 8, 64.3% of the QP sample satisfies this more stringent criterion, indicating the effectiveness of our selection and providing a more reliable subset for further analysis of physically bound quasar pairs.

## 5. SUMMARY

In this study, we systematically searched for quasar pairs using the DESI DR1 quasar catalog. By applying redshift-dependent angular separation limits and a velocity threshold of 2000 km/s, we identified 1,842 candidate quasar pairs. Through visual inspection of both imaging and spectral data, we classified the systems into four categories. Our key findings include:

- A significant concentration of quasar pairs within  $z \sim 1-2.5$ , consistent with pre-merger scenarios.
- A nearly flat projected separation distribution beyond 20 kpc, suggesting a long-lived pre-merger phase.

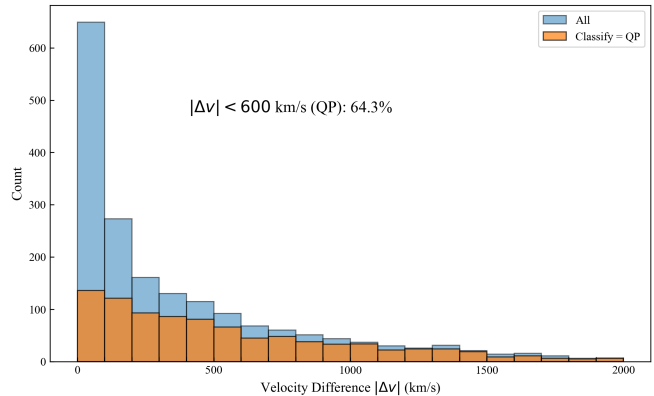


**Figure 8.** Distribution of line-of-sight velocity differences  $|\Delta v|$  for all quasar pairs (blue) and those classified as QP (orange). The horizontal axis shows  $|\Delta v|$  in km/s, and the vertical axis indicates the number of systems. A significant fraction (64.3%) of QP systems exhibit  $|\Delta v| < 600$  km/s, suggesting that most selected pairs are likely to be physically associated, and providing a refined subsample for studies of dual AGN dynamics.

- A refined QP sample where 64.3% of the pairs have  $|\Delta v| < 600$  km/s, increasing the likelihood of physical association.

The resulting catalog represents one of the largest spectroscopically confirmed samples of quasar pairs to date, offering a valuable resource for investigating SMBH co-evolution, gravitational lensing, and the assembly of large-scale structures.

## DATA AVAILABILITY

The quasar pair catalog in this work is available and can be downloaded in [https://github.com/astroliang/DESI\\_DR1\\_QP](https://github.com/astroliang/DESI_DR1_QP)

## ACKNOWLEDGMENTS

Qihang Chen should be viewed as the co-first author.

This research uses services or data provided by the SPectra Analysis and Retrieval Catalog Lab (SPARCL) and the Astro Data Lab, which are both part of the Community Science and Data Center (CSDC) program at NSF’s National Optical-Infrared Astronomy Research Laboratory. NOIRLab is operated by the Association of Universities for Research in Astronomy (AURA), Inc. under a cooperative agreement with the National Science Foundation.

The DESI Legacy Imaging Surveys consist of three individual and complementary projects: the Dark Energy Camera Legacy Survey (DECaLS), the Beijing-Arizona Sky Survey (BASS), and the Mayall z-band Legacy Survey (MzLS). Pipeline processing and analyses of the data were supported by NOIRLab and the Lawrence Berkeley

National Laboratory (LBNL). Legacy Surveys was supported by: the Director, Office of Science, Office of High Energy Physics of the U.S. Department of Energy; the National Energy Research Scientific Computing Center, a DOE Office of Science User Facility; the U.S. National Science Foundation, Division of Astronomical Sciences;

the National Astronomical Observatories of China, the Chinese Academy of Sciences and the Chinese National Natural Science Foundation. LBNL is managed by the Regents of the University of California under contract to the U.S. Department of Energy.

*Facilities:* DESI, DESI Legacy Survey

## REFERENCES

- 2025, arXiv e-prints, arXiv:2503.14745,  
doi: [10.48550/arXiv.2503.14745](https://doi.org/10.48550/arXiv.2503.14745)
- Abdurro'uf, Accetta, K., Aerts, C., et al. 2022, ApJS, 259, 35, doi: [10.3847/1538-4365/ac4414](https://doi.org/10.3847/1538-4365/ac4414)
- Agazie, G., Anumalapudi, A., Archibald, A. M., et al. 2023, ApJL, 952, L37, doi: [10.3847/2041-8213/ace18b](https://doi.org/10.3847/2041-8213/ace18b)
- Barnes, J. E., & Hernquist, L. 1996, ApJ, 471, 115, doi: [10.1086/177957](https://doi.org/10.1086/177957)
- Barnes, J. E., & Hernquist, L. E. 1991, ApJL, 370, L65, doi: [10.1086/185978](https://doi.org/10.1086/185978)
- Barrows, R. S., Comerford, J. M., Stern, D., & Assef, R. J. 2023, ApJ, 951, 92, doi: [10.3847/1538-4357/acd2d3](https://doi.org/10.3847/1538-4357/acd2d3)
- Blecha, L., Snyder, G. F., Satyapal, S., & Ellison, S. L. 2018, MNRAS, 478, 3056, doi: [10.1093/mnras/sty1274](https://doi.org/10.1093/mnras/sty1274)
- Capelo, P. R., Dotti, M., Volonteri, M., et al. 2017, MNRAS, 469, 4437, doi: [10.1093/mnras/stx1067](https://doi.org/10.1093/mnras/stx1067)
- Capelo, P. R., Volonteri, M., Dotti, M., et al. 2015, MNRAS, 447, 2123, doi: [10.1093/mnras/stu2500](https://doi.org/10.1093/mnras/stu2500)
- Chen, N., Di Matteo, T., Ni, Y., et al. 2023, MNRAS, 522, 1895, doi: [10.1093/mnras/stad834](https://doi.org/10.1093/mnras/stad834)
- Chen, Q., Jing, L., Zhu, X., et al. 2025, arXiv e-prints, arXiv:2504.17777, doi: [10.48550/arXiv.2504.17777](https://doi.org/10.48550/arXiv.2504.17777)
- Comerford, J. M., Pooley, D., Barrows, R. S., et al. 2015, ApJ, 806, 219, doi: [10.1088/0004-637X/806/2/219](https://doi.org/10.1088/0004-637X/806/2/219)
- Cox, T. J., Jonsson, P., Somerville, R. S., Primack, J. R., & Dekel, A. 2008, MNRAS, 384, 386, doi: [10.1111/j.1365-2966.2007.12730.x](https://doi.org/10.1111/j.1365-2966.2007.12730.x)
- Dawes, C., Storfer, C., Huang, X., et al. 2023, ApJS, 269, 61, doi: [10.3847/1538-4365/ad015a](https://doi.org/10.3847/1538-4365/ad015a)
- De Rosa, A., Vignali, C., Husemann, B., et al. 2018, MNRAS, 480, 1639, doi: [10.1093/mnras/sty1867](https://doi.org/10.1093/mnras/sty1867)
- De Rosa, A., Vignali, C., Severgnini, P., et al. 2023, MNRAS, 519, 5149, doi: [10.1093/mnras/stac3664](https://doi.org/10.1093/mnras/stac3664)
- DESI Collaboration, Aghamousa, A., Aguilar, J., et al. 2016, arXiv e-prints, arXiv:1611.00036, doi: [10.48550/arXiv.1611.00036](https://doi.org/10.48550/arXiv.1611.00036)
- DESI Collaboration, Abareshi, B., Aguilar, J., et al. 2022, AJ, 164, 207, doi: [10.3847/1538-3881/ac882b](https://doi.org/10.3847/1538-3881/ac882b)
- DESI Collaboration, Adame, A. G., Aguilar, J., et al. 2023, arXiv e-prints, arXiv:2306.06308, doi: [10.48550/arXiv.2306.06308](https://doi.org/10.48550/arXiv.2306.06308)
- Dey, A., Schlegel, D. J., Lang, D., et al. 2019, AJ, 157, 168, doi: [10.3847/1538-3881/ab089d](https://doi.org/10.3847/1538-3881/ab089d)
- Heckman, T. M., & Best, P. N. 2014, ARA&A, 52, 589, doi: [10.1146/annurev-astro-081913-035722](https://doi.org/10.1146/annurev-astro-081913-035722)
- Hennawi, J. F., Strauss, M. A., Oguri, M., et al. 2006, AJ, 131, 1, doi: [10.1086/498235](https://doi.org/10.1086/498235)
- Hennawi, J. F., Myers, A. D., Shen, Y., et al. 2010, ApJ, 719, 1672, doi: [10.1088/0004-637X/719/2/1672](https://doi.org/10.1088/0004-637X/719/2/1672)
- Hopkins, P. F., Hernquist, L., Cox, T. J., et al. 2005, ApJ, 630, 705, doi: [10.1086/432438](https://doi.org/10.1086/432438)
- Hou, M., Li, Z., & Liu, X. 2020, ApJ, 900, 79, doi: [10.3847/1538-4357/aba4a7](https://doi.org/10.3847/1538-4357/aba4a7)
- Hou, M., Liu, X., Guo, H., et al. 2019, ApJ, 882, 41, doi: [10.3847/1538-4357/ab3225](https://doi.org/10.3847/1538-4357/ab3225)
- Hwang, H.-C., Shen, Y., Zakamska, N., & Liu, X. 2020, ApJ, 888, 73, doi: [10.3847/1538-4357/ab5c1a](https://doi.org/10.3847/1538-4357/ab5c1a)
- Ji, X., Zheng, Z.-Y., Lin, R.-Q., & Feng, H.-C. 2024, arXiv e-prints, arXiv:2412.08397, doi: [10.48550/arXiv.2412.08397](https://doi.org/10.48550/arXiv.2412.08397)
- Kelley, L. Z., Blecha, L., & Hernquist, L. 2017, MNRAS, 464, 3131, doi: [10.1093/mnras/stw2452](https://doi.org/10.1093/mnras/stw2452)
- Koss, M., Mushotzky, R., Treister, E., et al. 2012, ApJL, 746, L22, doi: [10.1088/2041-8205/746/2/L22](https://doi.org/10.1088/2041-8205/746/2/L22)
- Levi, M., Bebek, C., Beers, T., et al. 2013, arXiv e-prints, arXiv:1308.0847, doi: [10.48550/arXiv.1308.0847](https://doi.org/10.48550/arXiv.1308.0847)
- Liu, X., Civano, F., Shen, Y., et al. 2013, ApJ, 762, 110, doi: [10.1088/0004-637X/762/2/110](https://doi.org/10.1088/0004-637X/762/2/110)
- Liu, X., Shen, Y., Strauss, M. A., & Greene, J. E. 2010, ApJ, 708, 427, doi: [10.1088/0004-637X/708/1/427](https://doi.org/10.1088/0004-637X/708/1/427)
- Liu, X., Shen, Y., Strauss, M. A., & Hao, L. 2011, ApJ, 737, 101, doi: [10.1088/0004-637X/737/2/101](https://doi.org/10.1088/0004-637X/737/2/101)
- Makarov, V. V., & Secrest, N. J. 2023, ApJS, 264, 4, doi: [10.3847/1538-4365/ac97f0](https://doi.org/10.3847/1538-4365/ac97f0)
- Mihos, J. C., & Hernquist, L. 1994, ApJL, 431, L9, doi: [10.1086/187460](https://doi.org/10.1086/187460)
- Mihos, J. C., & Hernquist, L. 1996, ApJ, 464, 641, doi: [10.1086/177353](https://doi.org/10.1086/177353)

- Müller-Sánchez, F., Comerford, J. M., Nevin, R., et al. 2015, *ApJ*, 813, 103, doi: [10.1088/0004-637X/813/2/103](https://doi.org/10.1088/0004-637X/813/2/103)
- Pfeifle, R. W., Weaver, K. A., Secrest, N. J., Rothberg, B., & Patton, D. R. 2024, arXiv e-prints, arXiv:2411.12799, doi: [10.48550/arXiv.2411.12799](https://doi.org/10.48550/arXiv.2411.12799)
- Pfeifle, R. W., Satyapal, S., Secrest, N. J., et al. 2019, *ApJ*, 875, 117, doi: [10.3847/1538-4357/ab07bc](https://doi.org/10.3847/1538-4357/ab07bc)
- Richards, G. T., Vanden Berk, D. E., Reichard, T. A., et al. 2002, *AJ*, 124, 1, doi: [10.1086/341167](https://doi.org/10.1086/341167)
- Satyapal, S., Secrest, N. J., Ricci, C., et al. 2017, *ApJ*, 848, 126, doi: [10.3847/1538-4357/aa88ca](https://doi.org/10.3847/1538-4357/aa88ca)
- Shen, Y., Liu, X., Greene, J. E., & Strauss, M. A. 2011, *ApJ*, 735, 48, doi: [10.1088/0004-637X/735/1/48](https://doi.org/10.1088/0004-637X/735/1/48)
- Van Wassenhove, S., Volonteri, M., Mayer, L., et al. 2012, *ApJL*, 748, L7, doi: [10.1088/2041-8205/748/1/L7](https://doi.org/10.1088/2041-8205/748/1/L7)
- Wu, Q., Scialpi, M., Liao, S., Mannucci, F., & Qi, Z. 2024, *A&A*, 692, A154, doi: [10.1051/0004-6361/202452291](https://doi.org/10.1051/0004-6361/202452291)
- Zou, H., Zhou, X., Fan, X., et al. 2017, *PASP*, 129, 064101, doi: [10.1088/1538-3873/aa65ba](https://doi.org/10.1088/1538-3873/aa65ba)